Catalysis Today xxx (2016) xxx–xxx

Contents lists available at ScienceDirect

Catalysis Today

journal homepage: www.elsevier.com/locate/cattod

Structured Reactors as an Alternative to Fixed-bed Reactors: Influence of catalyst preparation methodology on the partial oxidation of ethanol

Clarissa P. Rodrigues[a], Elka Kraleva[b], Heike Ehrich[b], Fabio B. Noronha[a,*]

[a] National Institute of Technology, Catalysis Division, Av. Venezuela 82, 20081-312 Rio de Janeiro, Brazil
[b] Leibniz Institute for Catalysis, Albert-Einstein-Str. 29a, Rostock, Germany

ARTICLE INFO

Article history:
Received 15 December 2015
Received in revised form 14 February 2016
Accepted 21 February 2016
Available online xxx

Keywords:
Bioethanol
Partial oxidation
Ni/CeSiOx catalyst
Hydrogen production
Monolithic reactors
Structured catalysts

ABSTRACT

This work studied the effect of the preparation of monolithic catalysts for partial oxidation of ethanol. Cordierite monoliths coated with 10Ni/$CeSiO_x$ catalyst were prepared by washcoating with two different binders (PVA and Ludox) and a direct sol–gel techniques. Scanning electron microscopy and transmission electron microscopy analyses and adherence tests revealed that structured washcoated monoliths prepared by the slurry with Ludox and direct synthesis using citrate method exhibited excellent dispersion and adherence of catalyst coatings. For the washcoated monolith obtained by slurry with PVA, large agglomerates of catalyst over the wall were observed. The tests with the monolith without catalyst revealed that POX of ethanol only takes place in the presence of the Ni-based catalysts. The monolith catalysts synthesized by slurry with Ludox and direct synthesis using citrate method exhibited a high formation of syngas. However, the preparation method of the monolithic catalysts affects product distribution at low temperature. The addition of Pt to the $NiCeSiO_x$ monolith catalyst synthesized by citrate method significantly improved the partial oxidation of ethanol reaction.

© 2016 Elsevier B.V. All rights reserved.

1. Introduction

Hydrogen production through ethanol conversion reactions has been extensively studied in the literature [1–7]. Different technologies can be used for the production of hydrogen from ethanol, including steam reforming (SR) (Eq. (1)), partial oxidation (POX) (Eq. (2)), and oxidative steam reforming (OSR) (Eq. (3)) [5]:

$$C_2H_5OH + 3H_2O \rightarrow 2CO_2 + 6H_2 \quad (1)$$

$$C_2H_5OH + 1.5O_2 \rightarrow 2CO_2 + 3H_2 \quad (2)$$

$$C_2H_5OH + (3-2x)H_2O + xO_2 \rightarrow 2CO_2 + (6-2x)H_20 \; < \; x \; < \; 0.5 \quad (3)$$

The partial oxidation (POX) of ethanol is an exothermic reaction that exhibits quick start-up and response times. Furthermore, the POX reactor is more compact than that of a steam reformer since the indirect addition of heat is not needed. Therefore, POX of ethanol provides the desired features for vehicle fuel cell applications [8]. In addition, POX of ethanol is also very attractive for solid oxide fuel cell (SOFC) because further purification steps are not required, which reduces the costs of the fuel processor [9,10].

Several catalysts have been studied for the POX of ethanol [8–18]. However, the majority of the studies about POX of ethanol used catalysts in powder form and fixed-bed reactors and then, hot-spot formation may occurs, which makes the reaction controll difficult. Alternatively, the monolithic structures can be used as a support to obtain catalytic reactors with high structural and thermal stability. Monolithic reactors offer the advantage of thin walls, high geometric surface area with enhanced heat and mass transfer, low pressure drop and rapid response to transient operations [19–21]. In addition, the easy scale-up and reduced costs of a compact catalyst design contribute to the large potential of monolith catalysts with respect to their application in hydrogen production technologies.

Monolithic catalyst is well known from automotive and industrial applications as exhaust gas converter. Structured reactors have been used for SR and OSR of ethanol [22–25] but their application for POX of ethanol is more scarce [19,20]. The extremely low contact time makes monoliths suitable for POX of ethanol at high temperature. Hotspots can be eliminated, improving the selectivity of the reaction. POX of ethanol was carried out on Co_3O_4/Al_2O_3 and NiO/Al_2O_3 catalysts washcoated on a cordierite monolith [19,20]. After 30 of time on stream (TOS), a large formation of carbon filaments was observed, which was responsible for catalyst degra-

* Corresponding author.
E-mail address: fabio.bellot@int.gov.brb (F.B. Noronha).

http://dx.doi.org/10.1016/j.cattod.2016.02.061
0920-5861/© 2016 Elsevier B.V. All rights reserved.

Please cite this article in press as: C.P. Rodrigues, et al., Structured Reactors as an Alternative to Fixed-bed Reactors: Influence of catalyst preparation methodology on the partial oxidation of ethanol, Catal. Today (2016), http://dx.doi.org/10.1016/j.cattod.2016.02.061

dation. Therefore, the development of stable structured catalysts for POX of ethanol at high temperature is still a challenge.

One crucial point for the development of structured reactors is the deposition of a suitable and stable catalytic layer on the ceramic support. The most known method to coat monolithic supports is the washcoating procedure, by dipping and removing the monolith from a solution containing the catalyst. It is probably the most versatile of the methods because any kind of solution can be applied, as suspension, colloidal or sol-gel containning the solid or precursors of catalysts. The characteristic of the final coating depends on the monolith properties, solution properties and preparation conditions [21,26]. Several parameters must be controlled for obtaining uniform, reproducible and mechanically stable washcoat; such as: pH of the solution, particle size, viscosity, slurry concentration, primers and binders used, etc.

For coating ready-made catalysts on a monolith, a slurry of particles with controlled size (about 5 μm) has to be used, with a properly solvent and a binder agent. The first step is to ball mill the ready catalyst to a small size, producing an easily accessible coat layer. According to the literature [21,27,28], the adhesion of the washcoated layer on the porous support is improved with the reduction of particle size down to colloidal dimensions. Another way to improve the catalyst adhesion is increasing the contact surface between the particles and the support, by binding agent addition. The binder is preferably colloidal silica or alumina, depending on the application. Alumina has the advantage that is more thermostable than silica, because high-temperature applications silica binder can be lost by steaming. It is worth noting that the binder must be made by the same material as the support, because it could influence the physical and acid/base properties of catalysts causing a strong influence on the catalytic performance. The amount of binder to be used is preferably kept minimal, even 1%wt of total solids is sufficient to properly attach the ready catalyst to the support, avoidding the coverage of active phase or channel blocking [27,29–31].

The aim of this work is to investigate the performance of $Ni/CeSiO_x$ and PtNi/CeSiOx washcoated monolithic catalyst for the POX of ethanol. The monolithic catalyst was prepared by two different methods: (i) the traditional dip-coating procedure for the monolith washcoat with addition of two different binders and (ii) the direct synthesis of the mixed oxide on the monolith itself by one step citrate route.

2. Material and methods

2.1. Catalyst preparation

$CeSiO_x$ catalyst support was synthesized by co-precipitation method. An aqueous solution of $Ce(NO_3)_3{\cdot}6H_2O$ (Sigma-Aldrich)(0.31 mol L^{-1}) was added to a suspension containing 3 g of SiO_2 (Aerosil 300) solubilized in a NaOH (Aldrich 98%) solution (C_{NaOH} = 0.34 mol L^{-1}) with continuous stirring at 840 rpm for 1 h. Finally, the solvent was removed by filtration and the solid was washed with hot water until reach pH 7. The solid was dried at 100 °C for 16 h and then, calcined at a heating rate of 1.7 °C min^{-1} from room temperature to 500 °C, and kept for 5 h in a muffle furnace. The nominal CeO_2:SiO_2 weight ratio is 8.6.

The $Ni/CeSiO_x$ catalyst in powder form was prepared by incipient wetness impregnation of the support $CeSiO_x$ with an aqueous solution of $Ni(NO_3)6H_2O$ (Sigma Aldrich) in order to obtain 10 wt.% of Ni. After impregnation, the samples were dried and calcined at the same thermal treatment described for the support. The final powder catalyst was sized in a particle range of 0.4–0.5 mm.

Monolithic catalysts were prepared using two different methods. The first one involved the washcoating by slurry, and the second one was the co-precipitation by citrate method. Before incorporation of catalyst into monoliths, they were washed in isopropanol, calcined for 2 h at 800 °C; and weighted for obtaining the start pure monolith amount. A commercial 400 cells per square inch (cpsi) cordierite monolith cylinder with a diameter of 2 cm and a length of 6 cm from Rauschert was used.

The $Ni/CeSiO_x$ catalyst prepared in powder form and two differente binders were used to investigate the effect of coating procedure on the dipcoating preparation method of monolithic catalyst. PVA (polyvinyl alcohol, 95%, hydrolyzed, average MW = 100.000, Fluka) or Ludox HS-40 (colloidal silica, 40 wt.% in water, Aldrich) were employed as a binder. For the preparation of the washcoat slurries, the catalyst in powder form was ground by hand into coarse powder (particle size < 100 μm) in a mortar and pestle. A suspension with 10 wt.% of catalyst and 5 wt.% of binder in distilled water was prepared. In the first step, the binder was dissolved in water in a 250 mL graduated bottle by stirring smoothly with a magnetic stir bar at 65 °C and 150 rpm for 3 h in a water bath, and left without stirring overnight (about 16 h). An homogeneous clear solution was obtained [32]. After dipcoating in the slurry containing the catalyst/binder and drying, the impregnated washcoats monoliths were calcined at a heating rate of 1.7 °C min^{-1} from room temperature to 500 °C, and kept for 5 h in a muffle furnace. The coating procedure was finished when the monolith contains 2 g of catalyst before monolith calcination.

A $NiCeSiO_x$ monolith catalyst was also prepared by the citrate method ($NiCeSiO_x$ (CM)). Citric acid was added to an aqueous solution that contained all the required precursor salts of the support $(NH_4)_2Ce(NO_3)_6$ and SiO_2 (Aerosil 300), in a 9:1CeO_2:SiO_2 weight ratio, and of the active phase $Ni(NO_3)_2{\cdot}6H_2O$ (Sigma Aldrich), as described elsewhere [9,10]. The final solution was stirred for 10 min, and then the temperature was raised to start boiling, which was continued for 30 min to form a homogeneous chelate between the metal cations and the citrate anions. Then the solution was concentrated by evaporation at 80 °C until a viscous liquid was obtained. After dipcoating the monolith into the suspension containing the catalyst and drying, the impregnated washcoated monolith was calcined. The coating procedure was finished when the monolith contains 2 g of catalyst before monolith calcination. Then, the monolithic catalyst was calcined following the same procedure previously described.

A $1Pt10NiCeSiO_x$ monolith catalyst was also prepared by citrate method ($PtNiSiO_x$ (CM)). In this case, an aqueous solution containing $Ni(NO_3)_2{\cdot}6H_2O$ (Sigma Aldrich) and 8 wt.% H_2PtCl_6 in water solution (Sigma Aldrich) was added to a citric acid aqueous solution with all the required ions of the support. The preparation method was similar to the one previously described.

2.2. Adhesion test

Catalyst layer adhesion to the monolith ceramic walls was tested with an ultrassonic bath treatment according to the method described elsewhere [33], to verify the weight loss caused by mechanical stress. After 10 min, the sample was dried and the weight loss measured.

2.3. Characterization

The specific surface area of the powder samples was measured by N_2 adsorption-desorption isotherms at −196 °C on an ASAP 2420 Micromeritics instrument. Prior to the measurements, the samples were dried at 100 °C for 24 h, and then, submitted to *in situ* treatment under vacuum at 350 °C. The specific area was calculated using the BET methodology.

The chemical composition of powder sample was determined on S8 Tiger Bruker wavelength dispersive X-ray fluorescence

Please cite this article in press as: C.P. Rodrigues, et al., Structured Reactors as an Alternative to Fixed-bed Reactors: Influence of catalyst preparation methodology on the partial oxidation of ethanol, Catal. Today (2016), http://dx.doi.org/10.1016/j.cattod.2016.02.061

spectrometer (WD-XRF) with a rhodium tube operated at 4 kW. The analyses were performed with samples (300 mg) in powder form using a semi-quantitative method (QUANT-EXPRES/Bruker).

X-ray powder diffraction pattern of the calcined samples were obtained using a D8 Advance Bruker diffractometer equipped with a CuKα radiation source (1.5406 Å) and a nickel filter, in a 2θ range of 10–120 at a scanning rate of 0.02/s and a scan time of 1 s/step. The X-ray tube voltage and current were set at 40 kV and 40 mA, respectively. The apparent crystallite size of $CeSiO_x$, NiO and Pt was calculated by using a Lorentzian curve with FWHM (2θ) defined as $(180/\pi)\lambda/\cos(\theta)$CS_L in TOPAS 4.2 (DIFFRAC-TOPAS/Bruker), where CS_L is a macros parameter.

High-resolution transmission electron microscopy (HR-TEM) was performed with an aberration-corrected JEM-ARM200F (JEOL, Corrector: CEOS) 200 kV transmission electron microscope. The microscope is equipped with a JED-2300 energy-dispersive X-ray-spectrometer (EDXS) for chemical analysis. The aberration corrected STEM imaging high-angle annular dark field (HAADF) and annular bright field (ABF) were performed with a spot size of approximately 0.13 nm, a convergence angle of 30–36°, and collection semi-angles for HAADF and ABF of 90–170 mrad and 11–22 mrad, respectively. For the TEM analysis the sample was deposited without any pretreatment onto a holey carbon supported Cu-grid (mesh 300) and then transferred into the microscope.

Scanning electron microscopy analysis in emission field (FEG-SEM) was performed in a Quanta 200 microscope (FEI) with maximum operating voltage of 20 kV. The images were acquired using EDT detector. Details of operating conditions for images acquisition, such as pressure, spot size and working distance (WD), and sample region extension observed are available in the micrographic bar presented here.

2.4. Catalytic tests

The monolithic catalysts were tested for the POX of ethanol at temperatures between 400 to 800 °C and atmospheric pressure. The operating temperature was regulated by a thermocouple inside the oven, which was placed closed to the reactor. A thermocouple was inserted into the center of the monolith to measure the reaction temperature. The samples were previously reduced under H_2/N_2 flow (10 vol.%, 100 mL min^{-1}) at 600 °C for 1 h, followed by a N_2 purge for 30 min at 600 °C.

In the standard test, a feed containing an oxygen-to-ethanol molar ratio of 0.75 was used. Ethanol was pumped at a constant rate of 10 g h^{-1} to the evaporator heated at 120 °C and then mixed with a stream of air (290 mL min^{-1}) and N_2 (100 mL min^{-1}) at a GHSV = 50 h^{-1}. The reactant composition in gas flow under normal conditions was Ethanol:O_2:N_2 = 16/12/72 vol%. The catalysts were tested step-wise at selected temperatures, maintaining the reaction for 2 h at each temperature to check for possible deactivation.

The composition of the inlet and outlet gas mixtures was frequently analyzed *on-line* using Shimadzu gas chromatographs equipped with FID and TCD detectors. The carbon balance was higher than 95% for all the catalytic systems tested. The products detected by gas chromatography were hydrogen, methane, carbon dioxide, carbon monoxide, ethylene, ethane and acetaldehyde. Conversion of ethanol was defined as the ratio of the consumed moles of ethanol to the moles of ethanol in the feed. The product distribution was defined as the ratio of moles of one product i to total moles of products in the effluent flow free of water, as previously described [16].

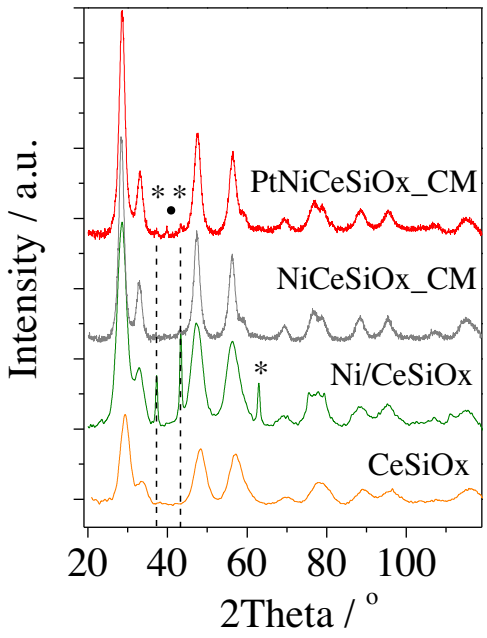

Fig. 1. Diffractograms of the CeSiOx (orange line) and Ni/$CeSiO_x$ (green line) powder samples and the NiCeSiOx (gray line) and PtNiCeSiOx (red line) citrate method powder sample. (*) NiO; (●) Pt. (For interpretation of the references to color in this subtitle, the reader is referred to the web version of this article.)

3. Results and discussions

3.1. Characterization of powder samples

The elemental composition of the calcined $CeSiO_x$ support and Ni/$CeSiO_x$ catalysts, their specific surface area and the XRD patterns were measured in the powder form. The chemical composition of the support agrees well with the nominal composition, which corresponds to 95 wt.% of Ce and 4.3 wt.% of Si. For the catalyst, the nickel content was about 14 wt.%. The specific surface area of the nickel catalysts (110 m^2g^{-1}) do not change significantly in comparison with the value of the $CeSiO_x$ support (127 m^2g^{-1}) (Table 1). As previously shown in the literature [34], doping CeO_2 with Si significantly increased the surface area, indicating high degree of incorporation of the Si into the CeO_2 structure. The diffractograms of the support and Ni-based catalysts are shown in Fig. 1. All samples exhibits the lines characteristic of CeO_2 with cubic phase [35]. In addition, the diffractogram of Ni/$CeSiO_x$ catalyst also shows the lines of NiO phase (2θ = 37.3°; 43.3°; 62.9°) [35]. For 10NiCeSiO$_x$ and PtNiCeSiOx powder prepared by citrate method, low intensity lines corresponding to NiO (2θ = 37.3°; 43.3°) were observed, suggesting the formation of small particles of NiO. The diffraction lines corresponding to metallic platinum were detected at 2θ = 39.4° and 81.38°.

The crystallite sizes of the $CeSiO_x$ and NiO phases estimated by Lorentzian curves are reported in Table 1. The Ni/$CeSiO_x$ prepared by incipient wetness impregnation of the support presents small

Table 1
Specific surface area of support and catalysts and crystallite sizes of $CeSiO_x$, NiO and Pt phases calculated by Scherrer equation.

Sample	Surface area (m^2 g^{-1})	Crystallite size (nm)		
		$CeSiO_x$	NiO	Pt
$CeSiO_x$	127	2.6	–	–
Ni/$CeSiO_x$	110	2.7	27.0	–
NiCeSiO$_x$ (CM)	123	5.4	2.3	–
PtNiSiO$_x$ (CM)	123	5.3	6.9	19.3

Please cite this article in press as: C.P. Rodrigues, et al., Structured Reactors as an Alternative to Fixed-bed Reactors: Influence of catalyst preparation methodology on the partial oxidation of ethanol, Catal. Today (2016), http://dx.doi.org/10.1016/j.cattod.2016.02.061

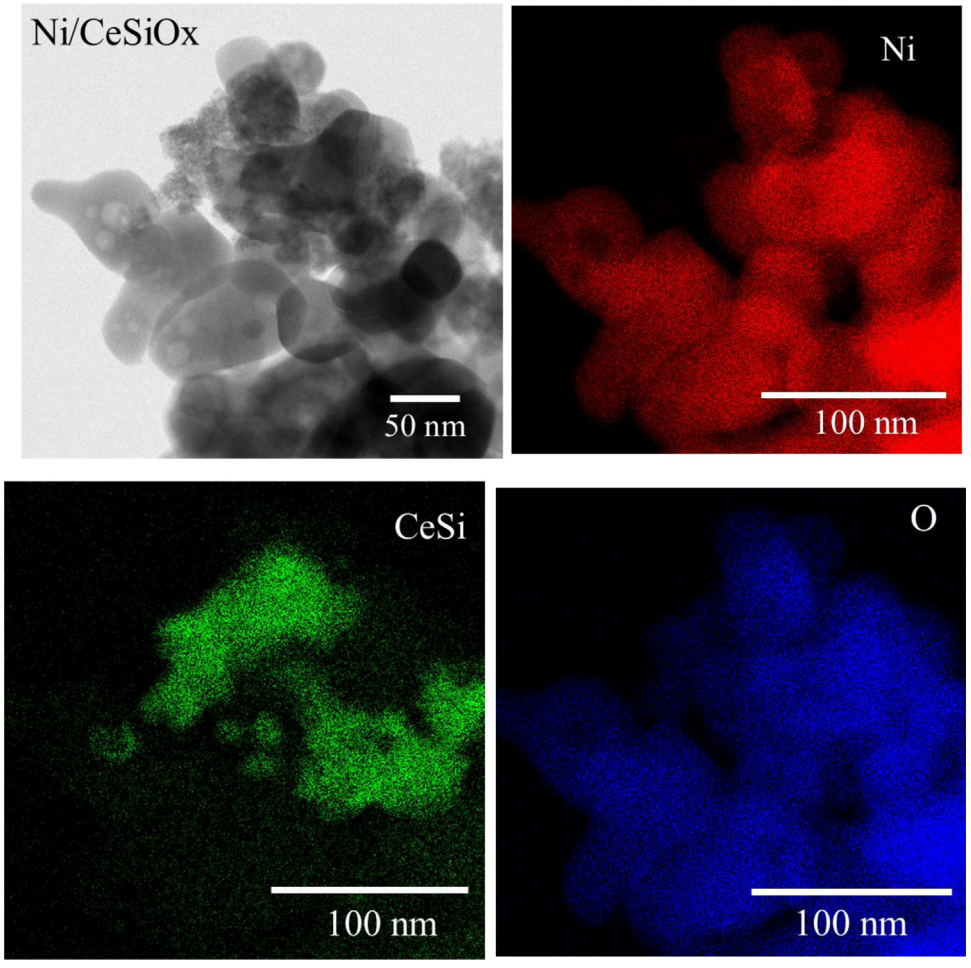

Fig. 2. STEM images of the Ni/CeSiO$_x$ powder catalyst. Element mapping of nickel, CeSi mixed oxide and oxygen in powder catalyst. (For interpretation of the references to color in the text, the reader is referred to the web version of this article.)

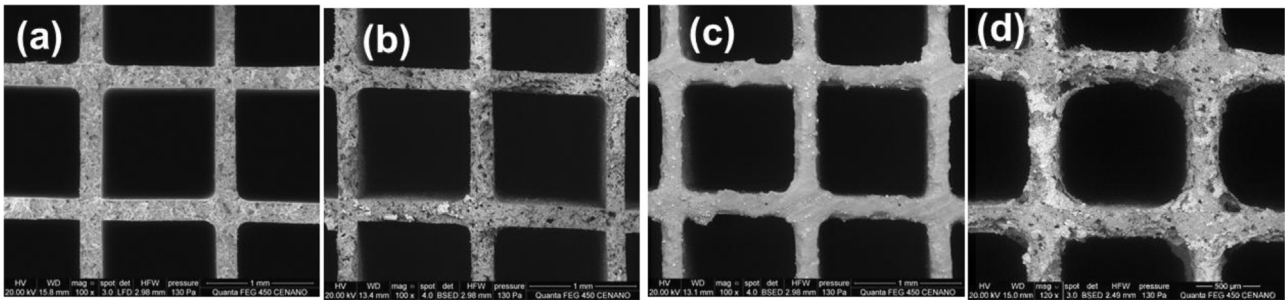

Fig. 3. FEG-SEM images of (a) uncoated cordierite monolith; (b) 10NiCeSiO$_x$ coated monolith with citrate method; (c) 10Ni/CeSiO$_x$ coated monolith with Ludox; (d) 10Ni/CeSiO$_x$ coated monolith with PVA.

ceria crystallite size (about 2.6 nm) and large NiO crystallites size (27.0 nm). Regarding the NiO crystallite size, the 10NiCeSiOx_CM exhibited smaller NiO crystallite size (2.3 nm) than Ni/CeSiO$_x$. The addition of Pt increased the NiO crystallite size. However, the citrate method led to smaller NiO crystallite size.

Fig. 2 presents STEM images of Ni/CeSiO$_x$ powder catalyst calcined at 500 °C. The micrographs clearly show large Ni particles (red) over the mixed oxide support (Ce-Si green and O blue). The elemental composition of the sample was confirmed by EDX measurements using a finely focused beam. According to element distribution, this catalyst consists of a small particles of Ce-Si mixed oxide support (5–10 nm) and large NiO particles (50–80 nm). These results are in agreement with XRF and XRD experiments.

3.2. Characterization of monolith catalysts

Table 2 presents the results obtained for coating procedure of monolith using the washcoating with a citrate solution and with a slurry contaning the ready-made catalyst and binder (Ludox or PVA). The monoliths were dipped vertically into the citric acid sol-gel solution and kept for 16 h and into the slurry for 10 min. This procedure was repeated until the increase in weight of the monolith achieves 2 g due to the addition of the coating material. Guiotto et al. [33], suggests that the precursor solution in the direct

Please cite this article in press as: C.P. Rodrigues, et al., Structured Reactors as an Alternative to Fixed-bed Reactors: Influence of catalyst preparation methodology on the partial oxidation of ethanol, Catal. Today (2016), http://dx.doi.org/10.1016/j.cattod.2016.02.061

Table 2
Amount of catalyst deposited on monolith after washcoating and the weight loss for the different washcoating procedures employing citric method, slurry with Ludox and slurry with PVA as a binder.

Sample		% Material washcoated	% weight loss
Citrate method	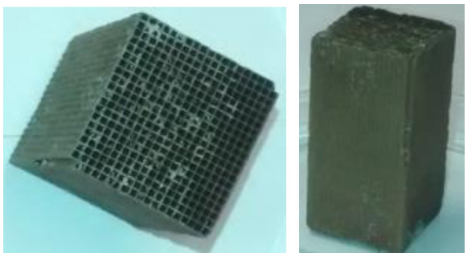	4.8	0.095
Ludox slurry	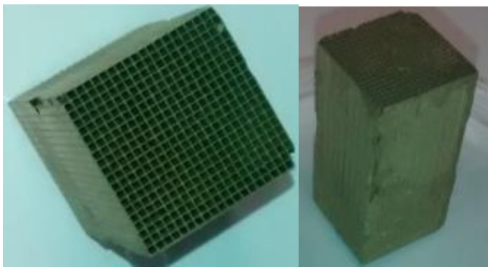	4.2	0.086
PVA slurry	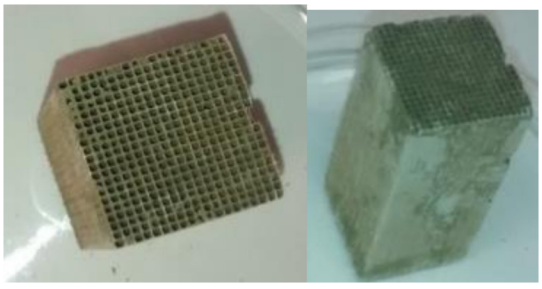	3.3	0.558

synthesis procedure needs to wet the supporting surface, beginning the deposition on the defects. The initial step of the deposition could be rather slow and difficult, due to preliminary diffusion of the precursors into the pore of the monolith. For this reason, the immersion step for citrate method was longer than the slurries washcoating.

After calcination at 500 °C, the amount of catalyst deposited during washcoating procedure was 0.77; 0.71 and 0.53 g for citrate method and for slurry with Ludox and PVA, respectively. The first characterization of the monolithic catalyst is visual. The images of the monolith obtained by citrate method and Ludox slurry show an uniform brown collored catalytic coating, while the image of the monolith prepared with PVA exhibits a non uniform collored coating distribution with some channels blockage.

The degree of adhesion of the catalytic layer was evaluated by measuring the sample weight loss after being immersed in isopropanol and exposed to ultrasonic vibration. After 10 min of exposure to mechanical vibrations, the washcoated monolith with citrate method, Ludox and PVA showed 0.095%; 0.086% and 0.558% of weight loss (Table 2), respectively, that correspond to a loss of 2% of material deposited for citrate method and Ludox and 17% for PVA. Similar weight loss is reported in the literature [27] for a monolith coated with 7% of zeolite BEA. The authors considered this loss very small, when compared with weight loss occurred for an uncoated cordierite monolith. PVA presented higher loss of the washcoating material due to a lower strenght of adhesion of the catalytic layer.

Cordierite monolith before and after washcoating procedure was sectioned in 2×2 cm small pieces, and they were characterized in a Quanta 200 microscope (FEI) both by backscattered and secondary electrons imaging and X-ray energy dispersive spectroscopy to investigate the distribution of coatings on monoliths wall, and the results are shown in Fig. 3. It is clear that the binder addition in the washcoat slurry cause an accumulation of the coating material inside the channels by the following order: Citrate Method (Fig. 3b) <Ludox (Fig. 3c) <PVA (Fig. 3d).

Fig. 4 shows the coating morphologies of the catalytic layers obtained by the different washcoating methods. Sol-gel solution allows to penetrate the defects of cordierite ceramic structure (Fig. 4(d–f)) where the surface cavities (black holes) could be clearly observed. This result suggests that a homogeneous thin cracked layer of a mixed oxide was formed over all cordierite support. For Ludox binder (Fig. 4g-i), it is observed that a thin layer with small particles was formed on the cordierite surface. For PVA, Fig. 4(j–l) shows a catalyst aglomeration and large particles of catalyst deposited in the ceramic surface. These results agree very well with the literature that reported the surface defects could be observed clearly on the channel walls, when the binder amount is less than 20%, [13].

In fact, according to Liu et al. [29] the degree of dispersion of the catalytic material particles in the washcoating solution affects the distribution of the catalytic layer on the surface of monolith. In addition, more homogeneous distribution of colloidal particles may help to form more uniform coating [33]. The slurry with Ludox led to a more homogeneous coating, with well dispersed particles, than the slurry with PVA.

Fig. 5 shows in detail one cordierite defect, which was washcoated with the slurry containing Ludox binder. According to literature [29], the penetration of small particles into monolith cavities leads to increase in the adherence of catalyst coating. This result is in agreement with the data of adhesion test (Table 2). Smaller weigth losses were observed for citrate method and Ludox slurry

Please cite this article in press as: C.P. Rodrigues, et al., Structured Reactors as an Alternative to Fixed-bed Reactors: Influence of catalyst preparation methodology on the partial oxidation of ethanol, Catal. Today (2016), http://dx.doi.org/10.1016/j.cattod.2016.02.061

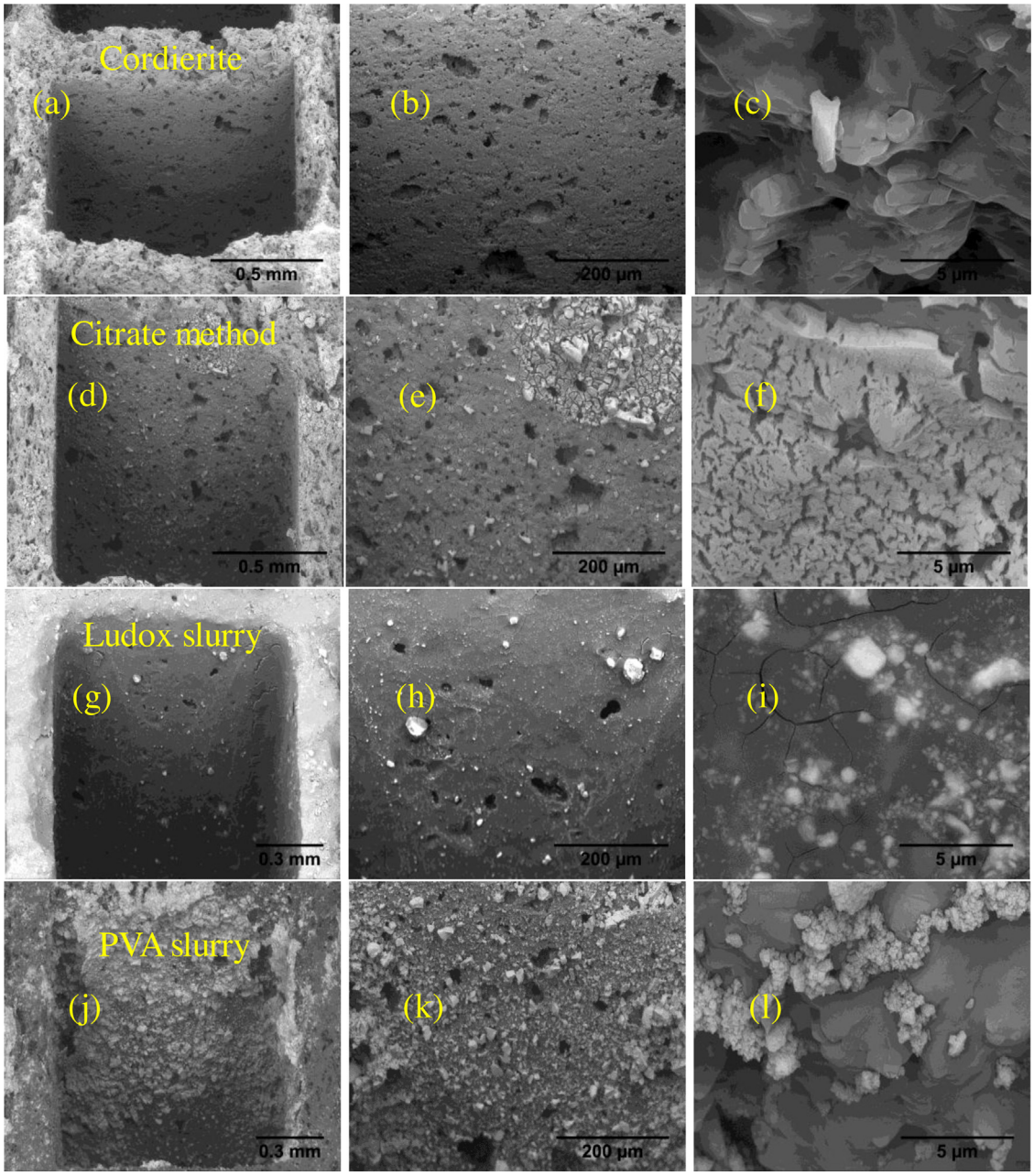

Fig. 4. FEG-SEM images of pure Cordierite monolith (200× (a); 500× (b); 20,000× (c)) and $NiCeSiO_x$ citrate method monolith (200x (d); 500× (e); 20,000× (f)) and $Ni/CeSiO_x$ Ludox slurry monolith (200x (g); 500× (h); 20,000× (i)) and $Ni/CeSiO_x$ PVA slurry monolith (200x (j); 500× (k); 20,000× (l)). (pressure: 130 Pa; spot size: 3.5; WD: 13.8 mm).

washcoated monoliths, that exhibits smaller particles in the coating layer. On the other hand, the large particles formed using PVA as a binder decreases the strenght of adhesion layer; forming an irregular coating and lowering the interaction among the particles in the slurry.

The spatial distribution of the coating elements within the monolith channel is also investigated by EDX mapping. It is important to stress that these areas were selected at positions far away from the meniscus, which develops at the corners of the monolith channels. At these positions the action of the suface tension forces that appear during the drying step of the slurry tends to concentrate the catalyst powders at values above the average on the rest of monolith walls [31]. The differences in the coated surface monoliths with various washcoating procedures are shown in Fig. 6. In principle, the direct synthesis (Fig. 6a) resulted in a more uniform and complete covering of the monolith. For Ludox slurry coating (Fig. 6b) it is possible to see the effect of surface tension forces, due to a large concentration of catalyst coating present at the channel outlet and the wall corner. The PVA slurry coating (Fig. 6c) exhibits the most heterogeneous catalyst layer, revealing the presence of regions (dark parts) with a little content of catalyst particles.

The element mapping of the monolith prepared by citrate method is presented in Fig. 7, which shows the pixels corresponding to aluminium (red) and magnesium (orange) from the monolithic support; to cerium (yellow), silicium (pink) and nickel (green) from the catalyst coating. From these results it is clear that the layer deposited on the surface is less compact and very thin, due to intense pixels to aluminium and magnesium elements from cordierite. Silicium signal shows two magnitude, one intense corresponding to the monolith surface composition, and other weak corresponding to the silicium element present in the mixed oxide. It is also interesting to note that there is an overlapping of nickel

Please cite this article in press as: C.P. Rodrigues, et al., Structured Reactors as an Alternative to Fixed-bed Reactors: Influence of catalyst preparation methodology on the partial oxidation of ethanol, Catal. Today (2016), http://dx.doi.org/10.1016/j.cattod.2016.02.061

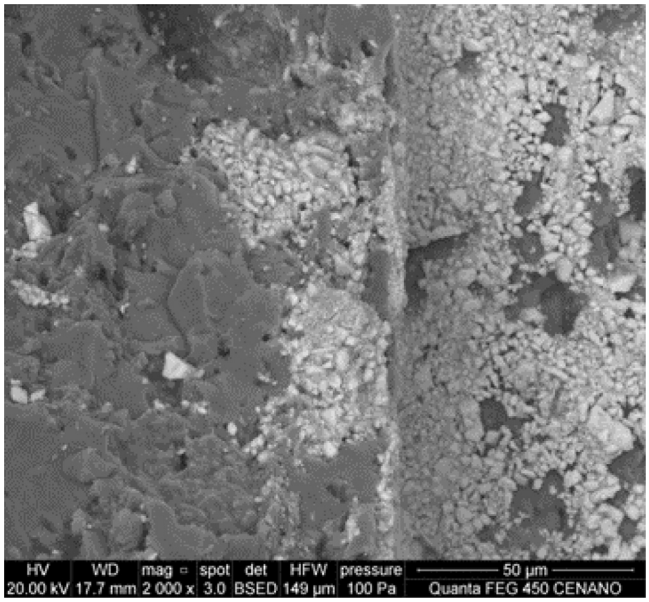

Fig. 5. Detail of cordierite cavity: penetration of catalyst small particles from the slurry with Ludox binder.

and cerium signals, suggesting that NiO layers are in contact with the surface of $CeSiO_x$ all over the monolith area.

The elements distribution for $Ni/CeSiO_x$ slurry Ludox coated monolith for one region with a good channel coverage by the catalyst particles is presented in Fig. 8. Unlike the previous sample, this one features large yellow, pink and green area where the signals overlap; corresponding to cerium, silicon and nickel elements present in the initial powder catalyst. Concerning the cordierite support, signals with weak intensity are observed for aluminium and magnesium elements, suggesting a good dispersion of $Ni/CeSiO_x$ catalyst over the monolith surface.

The element mapping of $Ni/CeSiO_x$ slurry PVA monolith is presented in Fig. 9. Some regions of the surface only show pixels corresponding to cordierite support elements (Al (red); Mg (orange); Si (pink)). It is possible to identify fewer black areas that correspond to $CeSiO_x$ aggregated particles of the catalyst. This results differs significantly from that ones corresponding to a more intermixed and homogeneous distribution of the others two types of washcoating procedures.

The element mapping of the $PtNiCeSiO_x$ monolith is presented in Fig. 10, which shows the pixels corresponding to aluminium (red) and magnesium (orange) from the monolithic support; to cerium (yellow), silicium (pink), nickel (green) and platinum (light cyan) from the catalyst coating. From these results it is clear that the layer deposited on the surface is more compact, due to less intense pixels related to aluminium and magnesium elements from cordierite. Silicium signal shows an intense magnitude corresponding to the element present in the mixed oxide because this is overlapping of cerium signal. It is also interesting to note that the nickel signal shows evidence that the NiO layer is in contact with the surface of $CeSiO_x$ all over the monolith area. Less intense pixels to platinum is observed, appearing as large, isolated, aggregates. The dimension of the individual crystallites of metallic paltinum phase, estimated by Lorentzian curve, was about 19 nm (Table 1).

Therefore, the characterization experiments of monolithic catalysts revealed that: (i) the amount of catalyst deposited on the monoliths and the degree of adhesion of the catalytic layer are determined by the preparation procedure employed; and (ii) the distribution of the catalytic layer on the surface of monolith

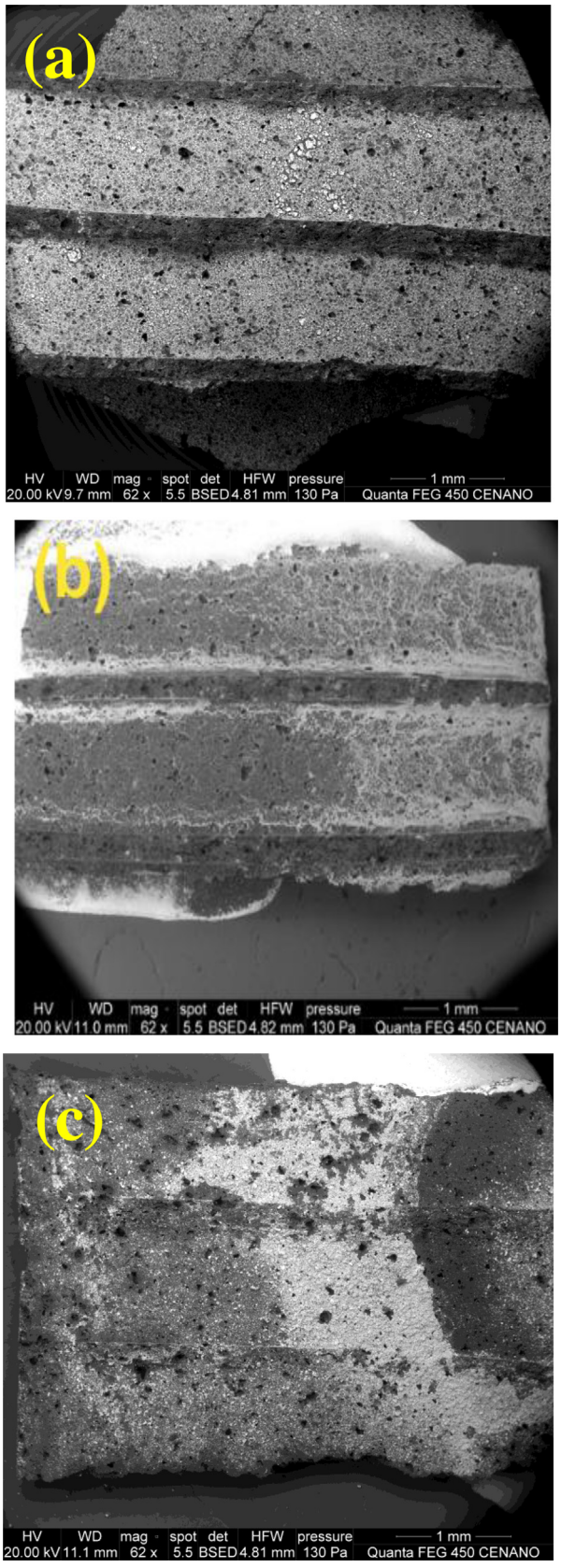

Fig. 6. FEG-SEM images of (a) $10NiCeSiO_x$ citrate method; (b) $10Ni/CeSiO_x$ Ludox slurry; (c) $10Ni/CeSiO_x$ PVA slurry monolith (Amplification: 60×).

Please cite this article in press as: C.P. Rodrigues, et al., Structured Reactors as an Alternative to Fixed-bed Reactors: Influence of catalyst preparation methodology on the partial oxidation of ethanol, Catal. Today (2016), http://dx.doi.org/10.1016/j.cattod.2016.02.061

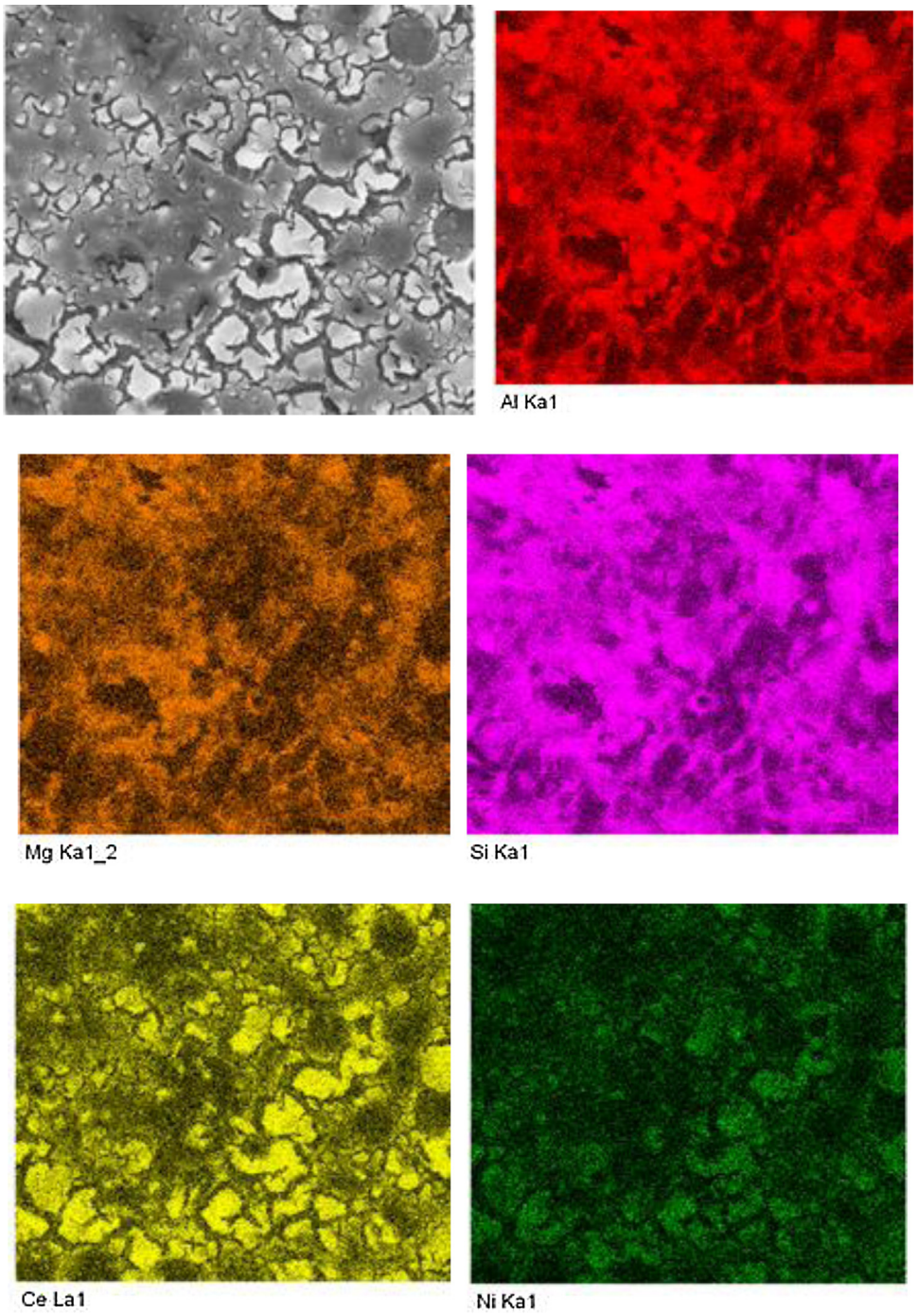

Fig. 7. Element mapping of aluminium, magnesium, cerium, silicium and n ickel on $NiCeSiO_x$ citrate method monolith. (For interpretation of the references to color in the text, the reader is referred to the web version of this article.)

strongly depend on the type of the binder used for preparation of washcoted slurry.

Since the monolithic catalysts prepared by the citrate and slurry with Ludox methods exhibited a more uniform, stable and complete covering of the monolith, they were tested on the POX of ethanol reaction.

3.3. Catalystic tests

For a better understanding of the catalytic processes occurring on monolith catalysts, ethanol conversion reaction was first performed for the monolith without any active materials under the conditions identical to those used in catalytic POX of ethanol. Ethanol conversion and products distribution for the non-catalytic oxidation of ethanol at different reaction temperatures are shown in Fig. 11. At 400 °C, ethanol conversion is low (<10%) and ethanol is only dehydrogenated to acetaldehyde and hydrogen (Eq. (4)) in the absence of catalyst. Increasing the temperature to 500 °C significantly increased ethanol conversion that achieved 100%. In addition, acetaldehyde is no longer observed and H_2, CO, and CH_4 were the main products formed. These results suggest that the homogeneous gas-phase reaction at low temperature is characterized by the dehydrogenation of ethanol to H_2 and acetaldehyde (Eq. (4)), which is decomposed to CO and CH_4 at temperatures above

Please cite this article in press as: C.P. Rodrigues, et al., Structured Reactors as an Alternative to Fixed-bed Reactors: Influence of catalyst preparation methodology on the partial oxidation of ethanol, Catal. Today (2016), http://dx.doi.org/10.1016/j.cattod.2016.02.061

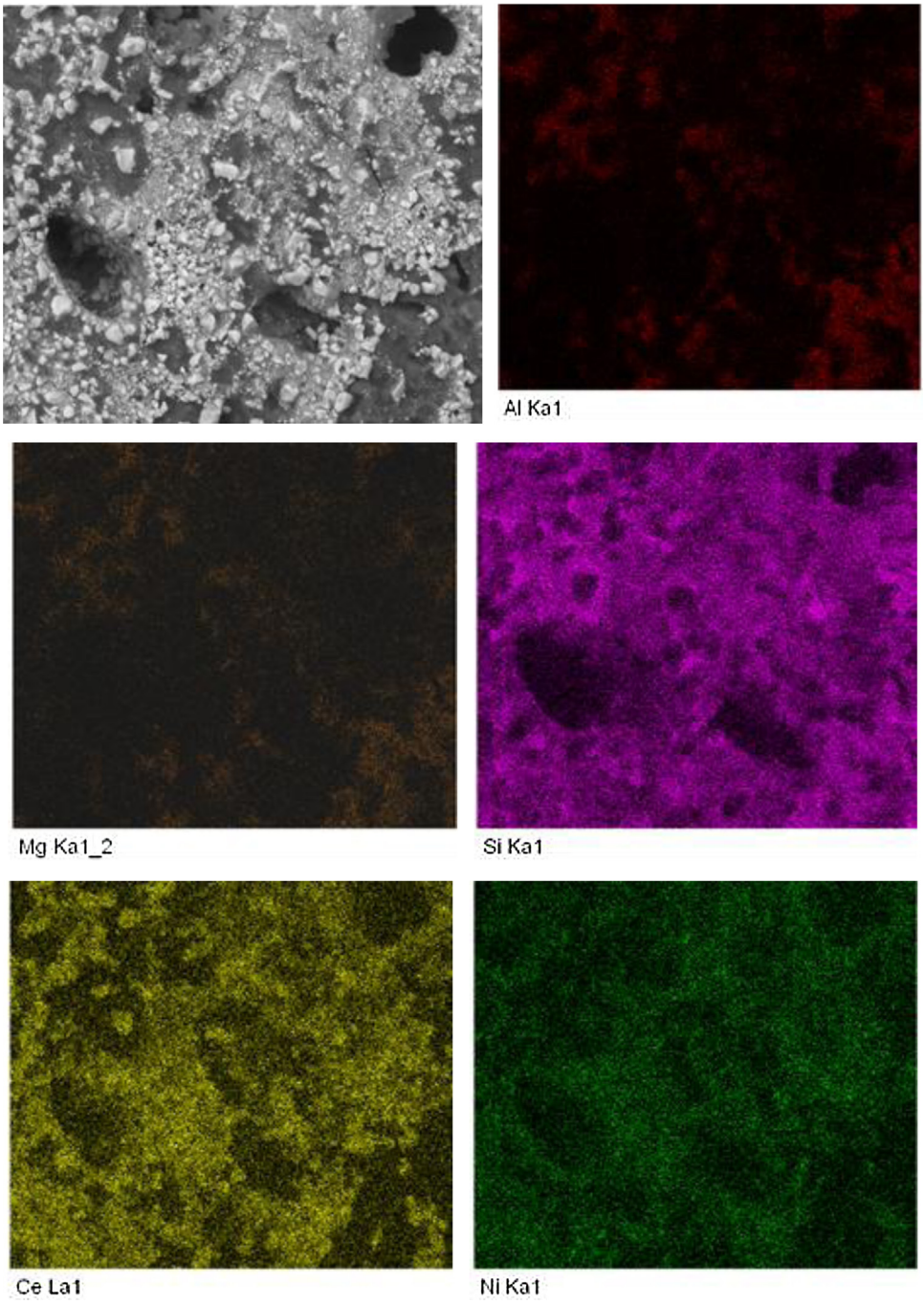

Fig. 8. Element mapping of aluminium, magnesium, cerium, silicium and nicke l on Ni/CeSiO$_x$ slurry Ludox monolith. (For interpretation of the references to color in the text, the reader is referred to the web version of this article.)

500 °C (Eq. (5)). Similar results were observed in the literature [20] employing cordierite monolith without catalyst layer, evidencing that the homogeneous gas phase reaction comprises the decomposition of ethanol. Only trace amount of CO_2 was detected, indicating that the water gas shift or combustion reactions does not occur in a significant extent in the absence of catalyst. Therefore, the POX of ethanol reaction did not take place in the whole range of studied temperatures on the pure monolith.

$$C_2H_5OH_{(g)} \rightarrow C_2H_4O_{(g)} + H_{2(g)} \quad (4)$$

$$C_2H_4O_{(g)} \rightarrow CH_{4(g)} + CO_{(g)} \quad (5)$$

In order to verify the potential of the monoliths washcoated as a catalyst for syngas production, the POX of ethanol was performed. The ethanol conversion and products distribution as a function of reaction temperature for monolithic catalysts prepared by citrate and slurry with Ludox methods are shown in Fig. 12(a) and (b), respectively. For both monoliths, H_2, CO_2, CO and CH_4 were the main products formed, indicating that POX of ethanol, water gas-shift and acetaldehyde decomposition reactions take place.

Increasing the reaction temperature increased ethanol conversion that was complete at 600 °C. Furthermore, the amount of H_2 and CO formed increased whereas the production of CO_2, acetaldehyde and ethylene decreased. At 600 °C, acetaldehyde and ethylene were no longer observed, and methane achieved a maximum formation. Further increase in the temperature favors the POX of ethanol reaction. The preparation method of the monolithic cata-

Please cite this article in press as: C.P. Rodrigues, et al., Structured Reactors as an Alternative to Fixed-bed Reactors: Influence of catalyst preparation methodology on the partial oxidation of ethanol, Catal. Today (2016), http://dx.doi.org/10.1016/j.cattod.2016.02.061

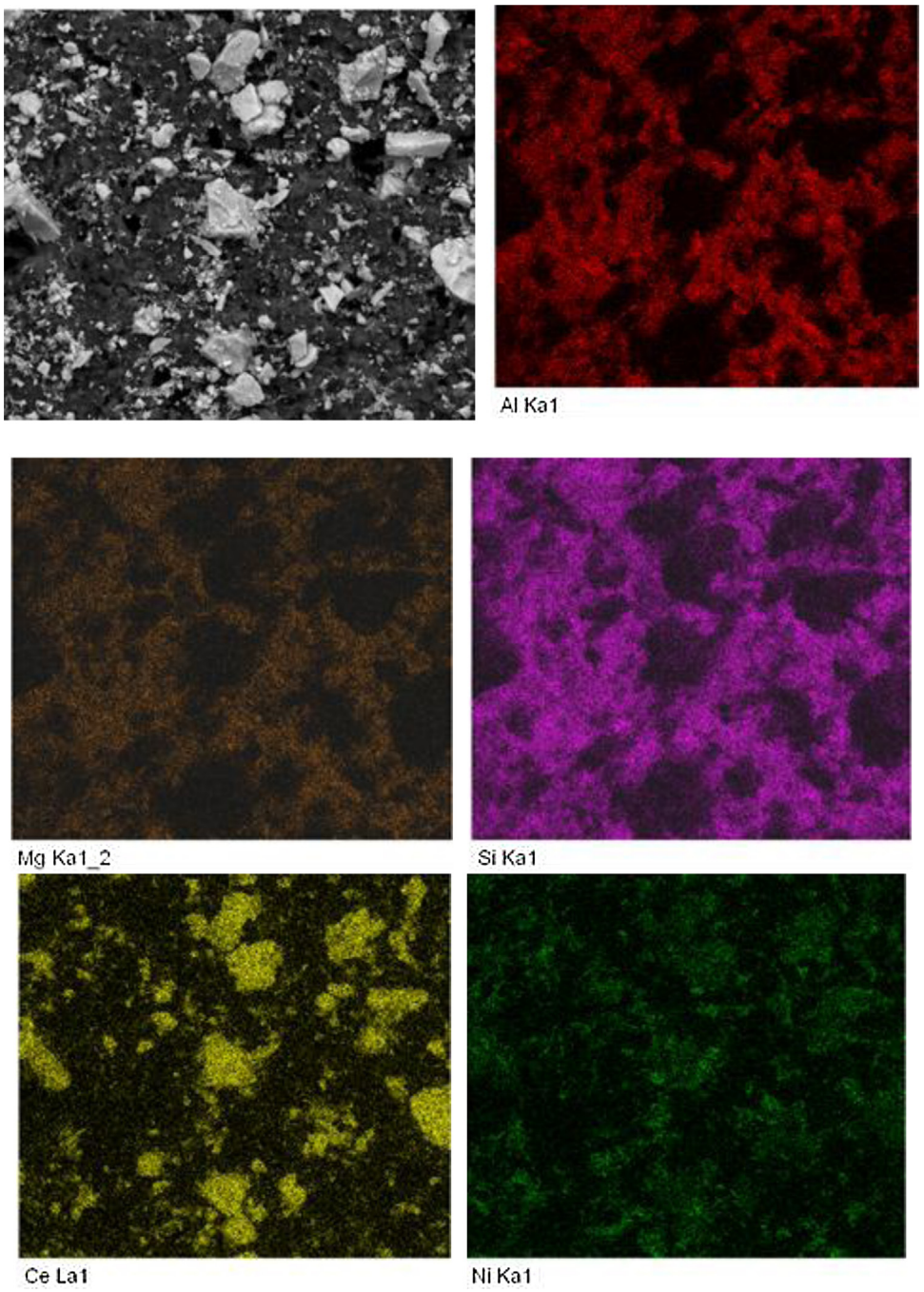

Fig. 9. Element mapping of aluminium, magnesium, cerium, silicium and nick el on Ni/CeSiO$_x$ slurry PVA monolith. (For interpretation of the references to color in the text, the reader is referred to the web version of this article.)

lysts affects product distribution at low temperature (500–600 °C). The monolithic catalyst prepared by citrate method exhibited a higher formation of H_2 and lower production of methane at this temperature range, indicating that POX of ethanol reaction is favored over this monolithic catalyst. This is likely due to the smaller NiO crystallite size of this catalyst as revealed by XRD.

Moreover, the addition of catalyst to the monolith increased the formation of H_2, CO and CO_2, promoting the POX of ethanol and WGS reactions instead of the decomposition reaction and inhibited the formation of acetaldehyde. Mattos and Noronha [8,12] reported that the POX of ethanol in the absence of catalyst led mainly to the formation of acetaldehyde, methane and ethylene. When the reaction was carried out over Pt/CeO_2 catalyst, the formation of acetaldehyde significantly decreased whereas the production of H_2 and CO increased. Based on TPD, TPSR and IR experiments, a mechanism for the POX of ethanol reaction was proposed. According to this mechanism, ethanol adsorbs as ethoxy species that can be dehydrogenated to acetaldehyde. This can be decomposed to CH_4 and CO or it can oxidized to acetate species by oxygen from the feed or the ceria support. The acetate species can be decomposed to CH_4, CO and/or oxidized to CO_2 via carbonate species. Our results are in agreement with the mechanism proposed in the literature.

In addition, the effect of Pt addition on the performance of NiCeSiO$_x$-CM monolithic catalyst (Fig. 12a) for POX of ethanol is investigated in the temperature range of 500–700 °C, and the results are presented in Fig. 13. The PtNiCeSiOx monolithic catalyst

Please cite this article in press as: C.P. Rodrigues, et al., Structured Reactors as an Alternative to Fixed-bed Reactors: Influence of catalyst preparation methodology on the partial oxidation of ethanol, Catal. Today (2016), http://dx.doi.org/10.1016/j.cattod.2016.02.061

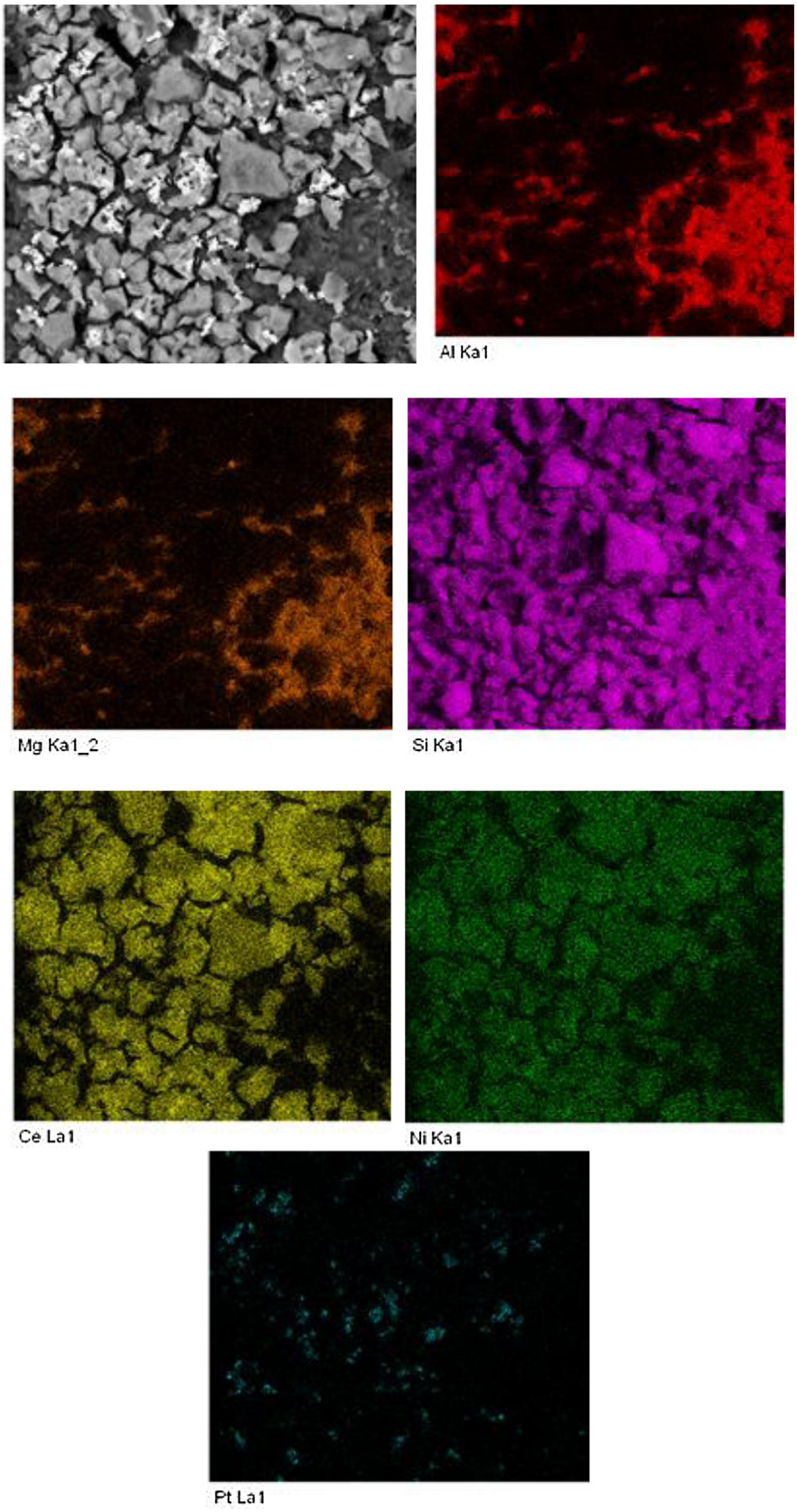

Fig. 10. Element mapping of aluminium, magnesium, cerium, silicium, nickel and platinum on Pt NiCeSiO$_x$ monolith. (For interpretation of the references to color in the text, the reader is referred to the web version of this article.)

Please cite this article in press as: C.P. Rodrigues, et al., Structured Reactors as an Alternative to Fixed-bed Reactors: Influence of catalyst preparation methodology on the partial oxidation of ethanol, Catal. Today (2016), http://dx.doi.org/10.1016/j.cattod.2016.02.061

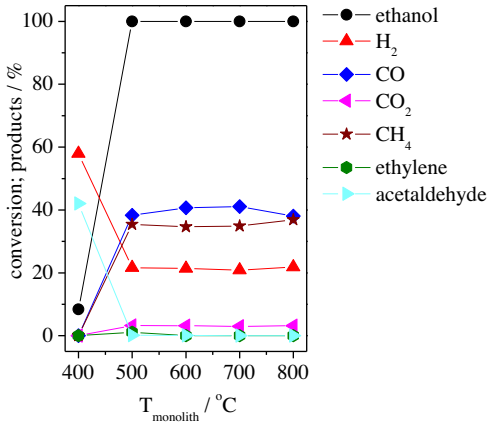

Fig. 11. Ethanol conversion and products distribution as a function of reaction temperature for POX of ethanol reaction over blank monolith (T = 400–8 00 °C; O_2/EtOH=0.75; P = 1 bar; GHSV = 50 h^{-1}).

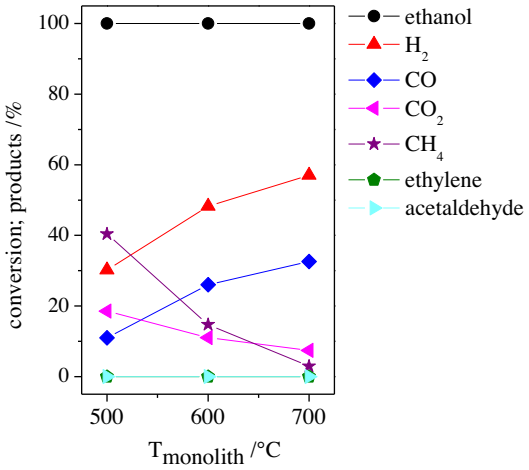

Fig. 13. Ethanol conversion and products distribution as a function of reaction temperature for $PtNiCeSiO_x$ _CM for POX of ethanol reaction (T = 600–8 00 °C; O_2/EtOH = 0.75; P = 1 bar, GHSV = 50 h^{-1}).

prepared by citrate method exhibited complete ethanol conversion at all reaction temperatures, and the main products were H_2, CO, CO_2 and CH_4. Increasing the temperature, significantly increased the formation of H_2 and CO whereas the production of methane and CO_2 decreased. Furthermore, acetaldehyde and ethylene were not formed even at 500 °C. A comparison between the product distribution obtained for the monometallic (Fig. 12a) and bimetallic (Fig. 13) monolithic catalysts reveals that Pt addition promoted the POX of ethanol reaction, reduced the production of methane and inhibited the formation of acetaldehyde. In addition, the highest syngas production occurs at high temperature (700 °C).

The type of the metal affects signficantly the mechanism of POX of ethanol [12–14]. Ru/Y_2O_3 catalyst showed a highest selectivity to syngas than Pd/Y_2O_3 catalyst for POX of ethanol at 800 °C. Oxidative dehydrogenation of ethanol to acetaldehyde was favored over Co/CeO_2 catalyst whereas ethanol decomposition took place over Pd/CeO_2 catalyst during POX of ethanol at low temperature (300 °C). These results were explained based on the reaction mechanism previously proposed [8]. Recently, we studied the effect of Pt addition to a Ni/CeO_2 catalyst for the low temperature steam reforming (LTSR) [36]. Mechanistic studies using mass spectroscopy and DRIFTS techniques revealed that Pt enhanced the decomposition rate of acetaldehyde, which could explain the absence of acetaldehyde formation on the bimetallic monolithic catalyst. Furthermore, the segregation of Pt on the surface of Ni particles promoted the decomposition of dehydrogenated and acetate species to hydrogen, methane, CO and carbonate species at low temperature. This might favor the syngas production at high temperature.

4. Conclusions

$Ni/CeSiO_x$ monolithic catalysts were successfully prepared employing the traditional dip-coating procedure with addition of Ludox binder and the direct synthesis of the mixed oxide in a single step through a citrate route. Both procedures resulted in an uniform and homogeneous catalyst layer with high adherence. The FEG-SEM microscopy revealed a good adherence and catalyst distribution over the monolith surface. For the washcoated monolith obtained by slurry with PVA, large agglomerates of catalyst over the wall were observed. The tests with the monolith without catalyst revealed that the homogeneous gas-phase reaction at low temperature is characterized by the dehydrogenation of ethanol to H_2 and acetaldehyde, which is decomposed to CO and CH_4 at high temperatures. The monolith catalysts synthesized by slurry with Ludox and direct synthesis using citrate method exhibited a high formation of syngas, indicating that POX of ethanol only takes place in the presence of the Ni-based catalysts.

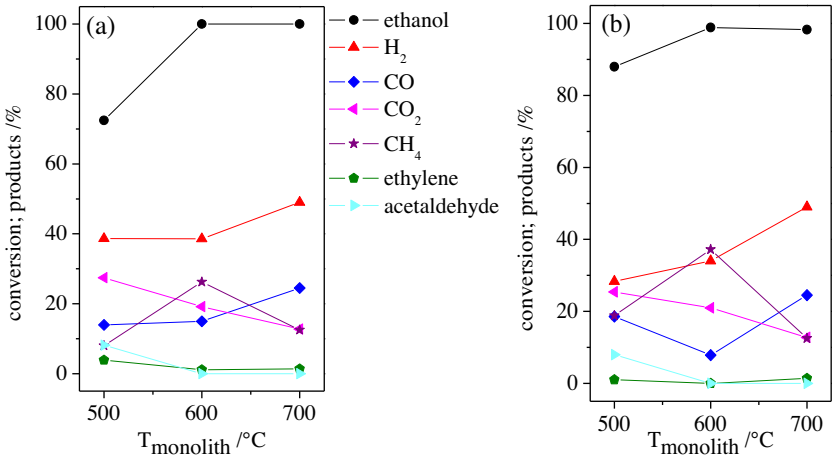

Fig. 12. Ethanol conversion and products distribution as a function of reaction temperature for monolithic catalysts prepared by (a) citrate method and (b) washcoating with Ludox slurry for POX of ethanol reaction (T = 500–700 °C; O_2/EtOH = 0.75; P = 1 bar, GHSV = 50 h^{-1}).

Please cite this article in press as: C.P. Rodrigues, et al., Structured Reactors as an Alternative to Fixed-bed Reactors: Influence of catalyst preparation methodology on the partial oxidation of ethanol, Catal. Today (2016), http://dx.doi.org/10.1016/j.cattod.2016.02.061

The preparation method of the monolithic catalysts affects product distribution at low temperature. The monolithic catalyst prepared by citrate method exhibited a higher formation of H_2 and lower production of methane at this temperature range, indicating that POX of ethanol reaction is favored over this monolithic catalyst. The addition of Pt to the $NiCeSiO_x$ monolith catalyst synthesized by citrate method significantly improved the partial oxidation of ethanol reaction.

Acknowledgements

Financial support of this work was provided by the DFG (GZ EH 477/1-1). The authors thank Dr. Marga-Martina Pohl from Likat for STEM-EDX measurements and comments, and Francisco Luiz Correa Rangel from DPCM/INT for FEG-SEM-EDX images and measurements.

Appendix A. Supplementary data

Supplementary data associated with this article can be found, in the online version, at http://dx.doi.org/10.1016/j.cattod.2016.02.061.

References

[1] A. Haryanto, S. Fernando, N. Murali, S. Adhikari, Energy Fuels 19 (2005) 2098–2106.
[2] P.D. Vaidya, A.E. Rodrigues, Chem. Eng. J. 117 (2006) 39–49.
[3] M. Ni, Y.C. Leung, M.K.H. Leung, Int. J. Hydrogen Energy 32 (2007) 3238–3247.
[4] P.R. de la Piscina, N. Homs, Chem. Soc. Rev. 37 (2008) 2459–2467.
[5] L.V. Mattos, G. Jacobs, B.H. Davis, F.B. Noronha, Chem. Rev. 112 (2012) 4094–4123.
[6] J.L. Contreras, J. Salmanes, J.A. Colin-Luna, L. Luno, B. Quintana, I. Cordova, B. Zeifert, C. Tapia, G.A. Fuentes, Int. J. Hydrogen Energy 39 (2014) 18835–18853.
[7] T. Hou, S. Zhang, Y. Chen, D. Wang, W. Cai, Renew. Sustain. Energy Rev. 44 (2015) 132–148.
[8] L.V. Mattos, F.B. Noronha, J. Catal. 233 (2005) 453–463.
[9] E. Kraleva, S. Sokolov, G. Nasillo, U. Bentrup, H. Ehrich, Int. J. Hydrogen Energy 39 (2014) 209–220.
[10] E. Kraleva, M.-M. Pohl, A. Jürgensen, H. Ehrich, Appl. Catal. B 179 (2015) 509–520.
[11] L.V. Mattos, F.B. Noronha, J. Power Sources 145 (2005) 10–15.
[12] L.V. Mattos, F.B. Noronha, J. Power Sources 152 (2005) 50–59.
[13] A.M. Silva, A.P.M.G. Barandas, L.O.O. Costa, L.E.P. Borges, L.V. Mattos, F.B. Noronha, Catal. Today 129 (2007) 297–304.
[14] A.M. Silva, L.O.O. Costa, A.P.M.G. Barandas, L.E.P. Borges, L.V. Mattos, F.B. Noronha, Catal. Today 133 (2008) 755–761.
[15] L.O.O. Costa, A.M. Silva, L.E.P. Borges, L.V. Mattos, F.B. Noronha, Catal. Today 138 (2008) 147–151.
[16] S.M. de Lima, I.O. da Cruz, G. Jacobs, B.H. Davis, L.V. Mattos, F.B. Noronha, J. Catal. 257 (2008) 356–368.
[17] A.M. Silva, A.M.D. de Farias, L.O.O. Costa, A.P.M.G. Barandas, L.V. Mattos, M.A. Fraga, F.B. Noronha, Appl. Catal. A 334 (2008) 179–186.
[18] S.M. de Lima, A.M. Silva, L.O.O. Costa, U.M. Graham, G. Jacobs, B.H. Davis, L.V. Mattos, F.B. Noronha, J. Catal. 268 (2009) 268–281.
[19] C.P. Rodrigues, V.T. da Silva, M. Schmal, Appl. Catal. B 96 (2010) 1–9.
[20] C.P. Rodrigues, M. Schmal, Int. J. Hydrogen Energy 36 (2011) 10709–10718.
[21] O. Sanz, F.J. Echave, F. Romero-Sarria, J.A. Odriozola, M. Montes, Advances in structured and microstructured catalystic reactors for hydrogen production, in: L.M. Gandía, G. Aramendi, P.M. Diéguez (Eds.), Renewable Hydrogen Technologies, Elsevier B.V., Oxford, 2013, pp. 201–224.
[22] D.K. Liguras, K. Goundani, X.E. Verykios, J. Power Sources 130 (2004) 30–37.
[23] A. Casanovas, C. Leitenburg, A. Trovarelli, J. Llorca, Catal. Today 138 (2008) 187–192.
[24] M. O'Connell, G. Kolb, K.-P. Schelhaas, M. Wichert, D. Tiemann, H. Pennemann, R. Zapf, Chem. Eng. Res. Design 90 (2012) 11–18.
[25] E. López, N.J. Divins, A. Anzola, S. Schbib, D. Borio, J. Llorca, Int. J. Hydrogen Energy 38 (2013) 4418–4428.
[26] D.M. Gómez, J.M. Gatica, J.C. Hernández-Garrido, G.A. Cifredo, M. Montes, O. Sanz, J.M. Rebled, H. Vidal, Appl. Catal. B 144 (2014) 425–434.
[27] T.A. Nijhuis, A.E.W. Beers, T. Vergunst, I. Hoek, F. Kapteijn, J.A. Moulijn, Catal. Rev. 43 (2001) 345–380.
[28] C. Agrafiotis, A. Tsetsekou, A. Ekonomaku, J. Mat. Sc. Lett. 18 (1999) 1421–1424.
[29] G. Liu, J. Guo, F. Meng, X. Zhang, L. Wang, Chinese J. Chem. Eng. 22 (2014) 875–881.
[30] L. Villegas, F. Masset, N. Guilhaume, Appl. Catal. A 320 (2007) 43–55.
[31] J.C. Hernández-Garrido, D. Gaona, D.M. Gómez, J.M. Gatica, H. Vidal, O. Sanz, J.M. Rebled, F. Peiró, J.J. Calvino, Catal. Today 253 (2015) 190–198.
[32] R. Zapf, C. Becker-Willinger, K. Berresheim, H. Bolz, H. Gnaser, V. Hessel, G. Kolb, P. Löb, A.-K. Pannwitt, A. Ziogas, Trans IChemE 81 (Part A) (2003) 721–729.
[33] M. Guiotto, M. Pacella, G. Perin, A. Iovino, N. Michelon, M.M. Natile, A. Glisenti, P. Canu1, Appl. Catal. A 499 (2015) 146–157.
[34] M.C. Ribeiro, G. Jacobs, B.H. Davis, L.V. Mattos, F.B. Noronha, Top. Catal. 56 (2013) 1634–1643.
[35] T.S. Moraes, R.C. Rabelo Neto, M.C. Ribeiro, L.V. Mattos, M. Kourtelesis, X. Verykios, F.B. Noronha, Top. Catal. 58 (2015) 281–294.
[36] T.S. Moraes, R.C. Rabelo Neto, M.C. Ribeiro, L.V. Mattos, M. Kourtelesis, S. Ladas, X. Verykios, F.B. Noronha, Appl. Catal. B 181 (2016) 754–768.

Please cite this article in press as: C.P. Rodrigues, et al., Structured Reactors as an Alternative to Fixed-bed Reactors: Influence of catalyst preparation methodology on the partial oxidation of ethanol, Catal. Today (2016), http://dx.doi.org/10.1016/j.cattod.2016.02.061